Correlation Effects in Two Electron Photoemission

F. O. Schumann, C. Winkler, and J. Kirschner

Max-Planck Institute of Microstructure Physics, Weinberg 2, 06120 Halle, Germany

(Received 26 March 2007; published 22 June 2007)

Many-body effects in solids are ultimately related to the correlation among electrons, which can be probed by double photoelectron emission. We have investigated the electron pair emission from a Cu(111) surface upon photon absorption. We are able to observe for the first time the full extension and shape of a depletion zone around the fixed emission direction of one electron. It has an angular extension of $\sim$1.2 rad, which is independent of the electron energy.

DOI: 10.1103/PhysRevLett.98.257604 PACS numbers: 79.60.−i, 73.20.At

Photoemission has become an indispensable tool to study the electronic properties of solids. Peaks in the angle-resolved energy distributions are usually associated with effective single-particle energies, which can be compared with band structure calculations. High-resolution photoemission has been able to discover effects of the electron-electron interaction or coupling to other degrees of freedom (e.g., phonons and spin waves). These show up as so-called kinks in the dispersion $E(k)$ curve [1]. A different and more direct approach to study the electron-electron interaction in solids is possible via double photoemission (DPE), which is the absorption of a single photon followed by the simultaneous emission of an electron pair. Within the dipole approximation, a noninteracting electron system has a vanishing DPE intensity; therefore, a finite DPE intensity requires a finite electron-electron interaction [2]. The mutual influence of the electron motion is the consequence of the Pauli principle and the Coulomb interaction. In fact, electrons tend to stay away from each other, thereby creating a zone of reduced electronic charge around each electron. This constitutes the concept of the exchange-correlation (XC) hole [3,4]. It is important to note that the XC hole also exists in momentum space [5]. The mutual influence among electrons is ultimately responsible for many-body effects such as magnetism, superconductivity, heavy fermions, etc. These ''highly correlated'' systems are the focus of intense research activities. The possibility to probe the XC hole via DPE exists, as a theoretical treatment for a Cu(100) surface showed [6]. This is beyond the capabilities of single photoemission. The experimental possibility to detect a finite DPE intensity from solids has been demonstrated previously [7–11]. In this Letter, we show for the first time that the technique of DPE has reached a status which allows the complete mapping of the XC hole. This is of fundamental interest for solid state theory; e.g., the XC hole is an integral part of the local density approximation, which is a widely used and a very successful description for solids [12]. We have studied a Cu(111) surface and found that the XC hole can be probed experimentally. It manifests itself as a depletion zone in the angular distribution of the intensity. More precisely, the emission direction of one electron is surrounded by a reduced intensity of the other electron. The size in angular space is $\sim$1.2 rad and independent of the kinetic energy of the electrons. We have therefore proven that the concept of the XC hole is an experimental reality.

Our experiment consists of 3 channel plate detectors; see Fig. 1. These ensure a large angular acceptance, which is in the drawing plane $\pm$1.57 rad; perpendicular to it, $\pm$0.4 rad is available. Delay line anodes allow the determination of the impact positions of electrons even if two electrons hit the same detector. These events we term as ''double hits,'' whereas we refer to ''single hits'' if the electrons are registered on different detectors. A pulsed photon source was provided by the synchrotron radiation facility in Berlin (BESSY II) operating in the single bunch mode; we used beam line TGM 4. The time period between light pulses is 800 ns, while the flight times for 5 and 20 eV electrons are 72 and 36 ns, respectively. The photon energy was set to 50 $\pm$ 0.2 eV. The propagation direction of the linear polarized light has an angle of 32° with respect to the surface normal. The polarization plane is in the drawing plane; see Fig. 1. The electron energies are determined via the flight times, where the time reference comes from the BESSY bunch marker. A coincidence circuit ensures that only electron pairs are detected. The ratio between true and

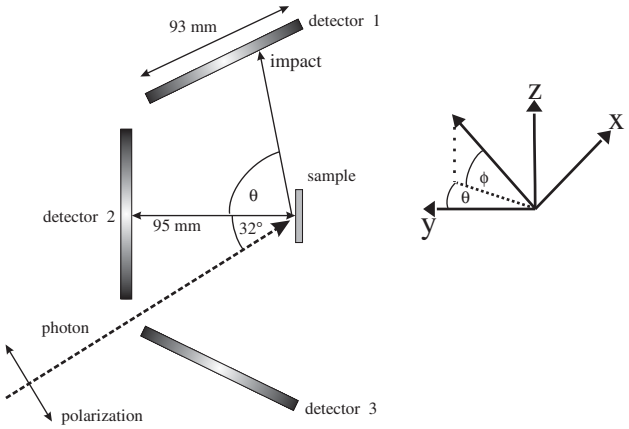

FIG. 1. Sketch of the experimental apparatus.

random coincidences is ≈ 1. The single count rate is about a factor of 500 higher than the coincidence count rate. The spectrometer is part of an ultrahigh vacuum system equipped with standard surface science tools. The impact positions are characterized by two angles measured with respect to the surface normal. The angle Θ is in the drawing plane of Fig. 1, while Φ is perpendicular to the drawing plane. Each coincident event is then characterized by 6 coordinates, namely, the individual energies and the pair of angles Θ and Φ. The total time resolution is approximately 1.4 ns. This will lead to an energy-dependent energy resolution, which is 1.5 eV for 20 eV electrons. We studied a clean and well-ordered Cu(111) surface, which was prepared via Ar sputtering and annealing up to 800 K. The experiments were performed at room temperature. The crystallographic $[\bar{2}11]$ axis is in the drawing plane of Fig. 1 and was fixed throughout the experiment.

In the case of double hits, a meaningful label is to term one electron "fast" and the other "slow" with the energies E_{fast} and E_{slow}, respectively. This implies that $E_{\text{fast}} > E_{\text{slow}}$; consequently we have to label single hits in the same fashion.

We display the resulting 2D energy distribution containing both contributions in Fig. 2. The bar on the panel defines the color code for the intensity, which is given in counts. Further, we added equidistant contours to the plot [13]. The onset of the DPE intensity occurs for a sum energy $E_{\text{sum}} = E_{\text{fast}} + E_{\text{slow}} \approx 40$ eV, which amounts to the photon energy minus twice the work function ($\approx$ 5 eV). If E_{sum} decreases from the maximum value, we note a steady increase of the intensity. For $E_{\text{fast}} > 20$ eV, most of the coincidence intensity is found for $E_{\text{slow}} <$ 10 eV. In other words, there is a preference of one electron being fast while the other is slow in this energy regime.

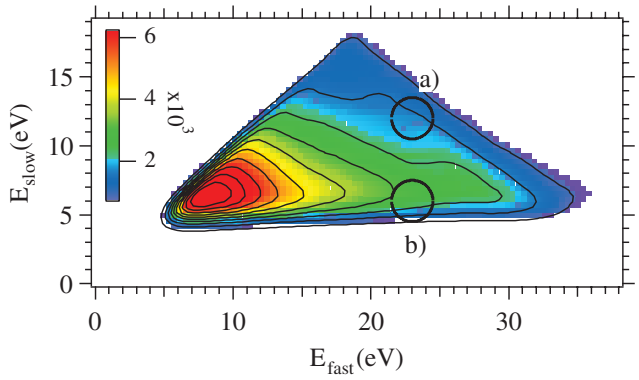

FIG. 2 (color). 2D energy distribution of the DPE intensity from a Cu(111) surface; the photon energy is 50 eV. One electron is termed fast, whereas the other is called slow, with energies $E_{\text{fast}} > E_{\text{slow}}$. The two circles with radius 1.5 eV indicate energy regions centered at $E_{\text{fast}} = 23$ eV ($E_{\text{slow}} = 12$ eV) and $E_{\text{fast}} = 23$ eV ($E_{\text{slow}} = 6$ eV). Coincident events within these windows are used for angular distributions of the coincidence intensity.

Individual 2D energy plots including only either single or double hits reveal that this is due to the contribution of double hits. Since those hits occur on the same detector, we know that the trajectories of these electrons must include smaller angles compared to single hits. This aspect will become important later on. The ratio of single to double hits is ≈ 6. A 2D angular presentation of our data requires the execution of several steps. First, we select values for E_{fast} and E_{slow}, respectively. In order to select enough coincidence events, we allow an uncertainty in the energy of ± 1.5 eV. This has been indicated by the circles drawn in Fig. 2. Now we can derive the angular distributions of the fast and slow electrons. These are not independent of each other, since electron pairs are detected. We emphasize that every fast electron has a slow counterpart. As an example, we show in Fig. 3 the angular distributions for fast and slow electrons centered at $E_{\text{fast}} = 23$ eV and $E_{\text{slow}} = 12$ eV [region (a) in Fig. 2]. Both distributions display the highest intensity if the electrons leave the sample along the surface normal. The intensity drops for increasing values of $|\Theta|$. The above energy selection for E_{fast} and E_{slow} focuses on the emission from the 3D states. Contributions from the Shockley surface state were too weak to be identified in our

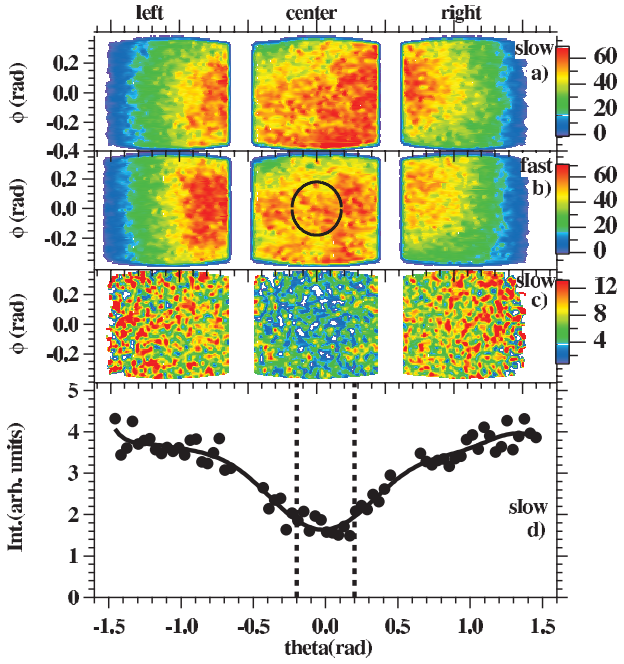

FIG. 3 (color). Angular distributions with $E_{\text{fast}} = 23$ eV and $E_{\text{slow}} = 12$ eV are displayed. (a) shows the 2D angular intensity for the slow electron, whereas in (b) the same for the fast electron is plotted. In (c), we plot the intensity for the slow electron if the fast electron is constrained to be within the area defined by the black circle of the center detector 2 in (b). From (c), a line scan can be computed, which is plotted in (d). The solid line is a guide to the eye, whereas the dashed vertical lines mark the boundary of the fixed direction. The intensity is given in counts, and the color code is on the right-hand side of the plot.

experiments. In the next step, we impose a geometrical constraint. We select only those fast electrons which leave the sample within a narrow angular direction. As an example, we have drawn a black circle in Fig. 3(b) which is centered at $\Theta = \Phi = 0$ rad. The emission direction is a cone with an angle of 0.18 rad, which is the radius of the circle in Fig. 3(b). In other words, we fix the direction of the fast electron and ask for the intensity of the slow electron around this direction. This is displayed in Fig. 3(c) after normalization to the intensity of the slow electron in Fig. 3(a). This procedure is necessary in order to take into account varying detection efficiencies. It is obvious that the intensity on the center detector is lower than on the left and right detectors.

To emphasize the point and to improve the statistics, we integrated the data along the Φ direction and show the resulting line scan along the Θ direction in Fig. 3(d). The vertical dashed lines mark the boundary of the allowed Θ values of the fast electron. The solid line through the data serves as a guide for the eye; the y axis is in arbitrary units as a result of our normalization procedure. We applied the same procedure for all line scans. Hence, direct comparison is possible. As already evident in Fig. 3(c), we observe that the fast electron is surrounded by a reduced slow electron intensity. We find that the intensity reaches a constant value at a radius $\Theta \sim 1.2$ rad, which is well inside the angular range of our experiment. This is the experimental manifestation of the exchange-correlation hole. Such a behavior was theoretically predicted for DPE from a Cu(100) surface [6]. The key observation is that we are able to show the full extension and shape of the depletion zone for the first time. It is, of course, possible to fix the emission direction of the slow electron and determine the intensity map of the fast electron. The result of such a presentation is qualitatively and quantitatively identical as far as the size of the depletion zone is concerned. The depletion zone could be observed for different values of E_{fast} and E_{slow}, where the size was independent of the selected energies. We will discuss below under which circumstances we observe an almost vanished depletion zone.

If we choose the fixed direction to be centered at $\Theta = 0$ rad, the maximum angle of the counterpart cannot exceed 1.57 rad if they are to leave the sample surface. However, it is possible to detect electron pairs whose trajectories include larger angles and to study the angular distribution. The significant advantage of our detection scheme is the ability to select the emission direction of one electron (either slow or fast) anywhere within the angular acceptance. We demonstrate this in Fig. 4. The fixed emission directions are defined by a circle in the 2D angular distribution equivalent to Fig. 3(b), which again has a radius of 0.18 rad. The center is at $\Theta = -1.0$ rad for Figs. 4(a) and 4(b); the case $\Theta = 1.0$ rad is depicted in Figs. 4(c) and 4(d). The vertical dashed lines in Figs. 4(b) and 4(d) mark the range of the allowed Θ values for the fixed electron. We lose the information of the intensity for Θ values on one side of the selected emission direction, but we gain a larger angular range on the other side. In other words, the maximum angle between the trajectories of the fixed fast and slow electrons is larger in this direction. Using the same procedure as before, we finally derive the 2D angular distribution of the slow electron around the fixed direction of the fast electron. These are plotted in Figs. 4(a) and 4(c). In the case of Fig. 4(a), we observe a low intensity on the left detector, if we move to the center detector the intensity has increased, and finally the intensity on the right detector is smaller than on the center detector. Again, improving the statistics via an integration along the Φ direction is appropriate and gives a more detailed view; the resulting line scan can be seen in Fig. 4(b). Two important observations can be made. First, we see that the intensity peaks at $\Theta \sim 0.2$ rad, while the "fixed" electron is centered at $\Theta \sim -1.0$ rad. This means that the angular size of the depletion zone is $\sim$1.2 rad, in line with the result shown in Fig. 3(d). More importantly,

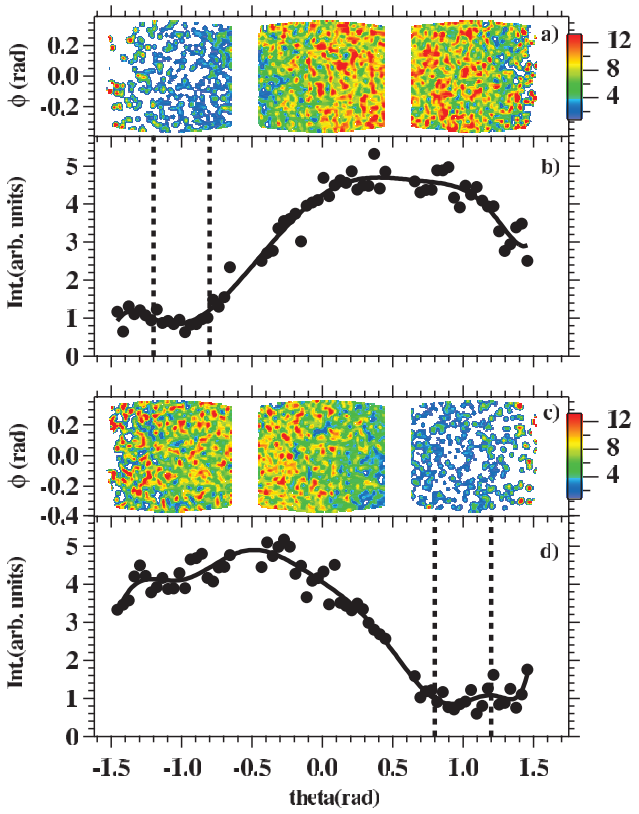

FIG. 4 (color). 2D angular distributions and resulting line scans are shown for electron pairs with $E_{\mathrm{fast}} = 23$ eV and $E_{\mathrm{slow}} = 12$ eV. The direction of the fixed fast electron is centered at either $\Theta = -1$ rad for (a) and (b) or $\Theta = 1$ rad for (c) and (d). The line scans of the intensity maps in (a) and (c) are plotted in (b) and (d), respectively. The solid lines are a guide to the eye, whereas the dashed vertical lines mark the boundaries of the fixed emission directions.

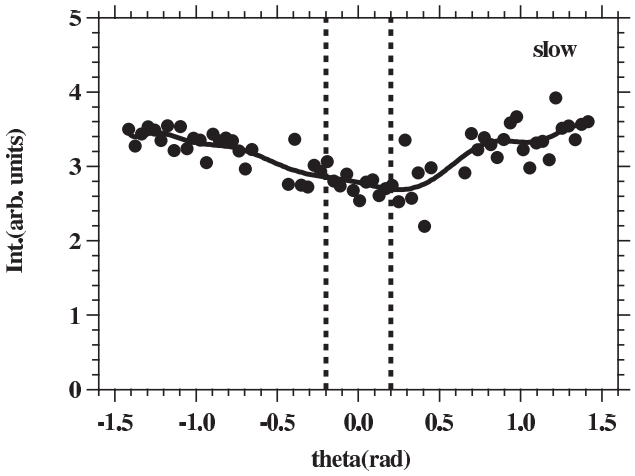

FIG. 5. Coincidence intensity for the slow electron if the direction of the fast electron is fixed at $\Theta = 0$ rad. We selected $E_{\text{fast}} = 23$ eV and $E_{\text{slow}} = 6$ eV. The solid line is a guide to the eye, whereas the dashed vertical lines mark the boundary of the fixed direction.

we see that the coincidence intensity drops off again if the angle between the two electrons is beyond ~1.2 rad. An equivalent situation is observed in Fig. 4(d) despite the breaking of symmetry. We have to emphasize that the photon beam hits the sample with an angle of 32°; see Fig. 1. Therefore, we cannot *a priori* expect to observe a symmetric behavior as we do. We can clearly see that the reduced intensity regime follows the fixed emission direction. The falloff of the coincidence intensity for large angles between the fast and slow electrons is expected, because ultimately two electrons are not correlated if they are well separated (in angular or momentum space).

Because of the size of the depletion zone, it is also justified to allow the fixed direction to be rather large. We have found no significant variation of the angular size of the depletion zone for other values of E_{fast} and E_{slow}. This means that in momentum space the depletion zone size will scale with the square root of the energy. It would be desirable to compare our experimental depletion zone size with theory. This is, however, beyond the capability of current solid state theory. Eventually, the comparison of theory and experiment of the depletion zone may lead to an improved description of the exchange-correlation hole in solids.

We would like to come back to the 2D energy distribution shown in Fig. 2. We have pointed out before that most of the coincidence intensity occurs for $E_{\text{slow}} < 10$ eV. This preference was mainly due to double hits. Detection on the same detector implicitly means that the trajectories of the electrons include small angles; hence, they are "close" to each other. If we select the energies centered at $E_{\text{fast}} = 23$ eV and $E_{\text{slow}} = 6$ eV [region (b) in Fig. 2], we are focusing on such events and ask how the angular distributions are affected. The result for the slow electron around the fixed direction of the fast electron is plotted in Fig. 5. We observe that the depletion zone has been "filled," and an almost constant intensity as a function of Θ is observed. This filling of the depletion zone occurs gradually if we vary E_{slow} from 12 to 6 eV. More specifically, the size of the depletion zone stays essentially constant, but the minimum is filled up. A simple picture of the electron-electron scattering, where the interaction between the electrons is mediated by the Coulomb interaction, shows that if the trajectories are forced to be close to each other, one electron is fast while the other is slow. In general, two electrons tend to avoid each other (due to the Pauli principle and Coulomb interaction), leading to the concept of the depletion zone. Our experiments confirm this picture as long as the individual energies E_{fast} and E_{slow} are not too unequal as just shown.

We conclude that we are able to fully map the depletion zone. This statement constitutes the major achievement of our work. We find for the depletion zone from electrons originating from a Cu(111) surface a size of ~1.2 rad independent of the energy of the electrons. We also discovered a correlation in energy space proven by an almost disappearing depletion zone if the electron energies are very unequal. The prospect of investigating the material dependence of the depletion zone is promising.

We acknowledge the expert assistance by H. Engelhard and D. Hartung. We thank the staff of the BESSY storage ring for excellent support.

[1] K. Byczuk, M. Kollar, K. Held, Y.-F. Yang, I. A. Nekrasov, T. Pruschke, and D. Vollhardt, Nature Phys. **3**, 168 (2007), and references therein.
[2] J. Berakdar, Phys. Rev. B **58**, 9808 (1998).
[3] E. Wigner and F. Seitz, Phys. Rev. **43**, 804 (1933).
[4] J. C. Slater, Rev. Mod. Phys. **6**, 209 (1934).
[5] P. Fulde, *Electron Correlations in Molecules and Solids*, Springer Series in Solid State Sciences Vol. 100 (Springer, Berlin, 1993).
[6] N. Fominykh, J. Berakdar, J. Henk, and P. Bruno, Phys. Rev. Lett. **89**, 086402 (2002).
[7] H. W. Biester, M. J. Besnard, G. Dujardin, L. Hellner, and E. E. Koch, Phys. Rev. Lett. **59**, 1277 (1987).
[8] R. Herrmann, S. Samarin, H. Schwabe, and J. Kirschner, Phys. Rev. Lett. **81**, 2148 (1998).
[9] F. U. Hillebrecht, A. Morozov, and J. Kirschner, Phys. Rev. B **71**, 125406 (2005).
[10] F. O. Schumann, C. Winkler, G. Kerherve, and J. Kirschner, Phys. Rev. B **73**, 041404(R) (2006).
[11] F. O. Schumann, J. Kirschner, and J. Berakdar, Phys. Rev. Lett. **95**, 117601 (2005).
[12] W. Kohn, Rev. Mod. Phys. **71**, 1253 (1999).
[13] In order to smooth the contour lines, we employed a Gaussian filter.